In summary, this study elucidated the precise binding mode of bacterial STING and the cognate ligand CDG by performing X-ray crystallography. The symmetrical interactions determine the specificity for CDG, which differs from the specificity for CDN of other STING complexes such as 2′3′-cGAMP. The crystal structures further provide a plausible mode of STING oligomerization, which is vital to STING's biological function. (Reported by Tzu-Ping Ko, Academia Sinica)

This report features the work of Yeh Chen and his colleagues published in Nat. Commun. ***13****, 26 (2022).*

TPS 05A Protein Microcrystallography
TPS 07A Micro-focus Protein Crystallography
TLS 15A1 Biopharmaceuticals Protein Crystallography

- X-ray Crystallography, Biological Macromolecules
- Protein Structures, Nucleotides, Viral Defense, Life Science

References

1. A. Millman, S. Melamed, G. Amitai, R. Sorek, Nat. Microbiol. **5**, 1608 (2020).
2. B. R. Morehouse, A. A. Govande, A. Millman, A. F. A. Keszei, B. Lowey, G. Ofir, S. Shao, R. Sorek, P. J. Kranzusch, Nature **586**, 429 (2020).
3. T.-P. Ko, Y.-C. Wang, C.-S. Yang, M.-H. Hou, C.-J. Chen, Y.-F. Chiu, Y. Chen, Nat. Commun. **13**, 26 (2022).

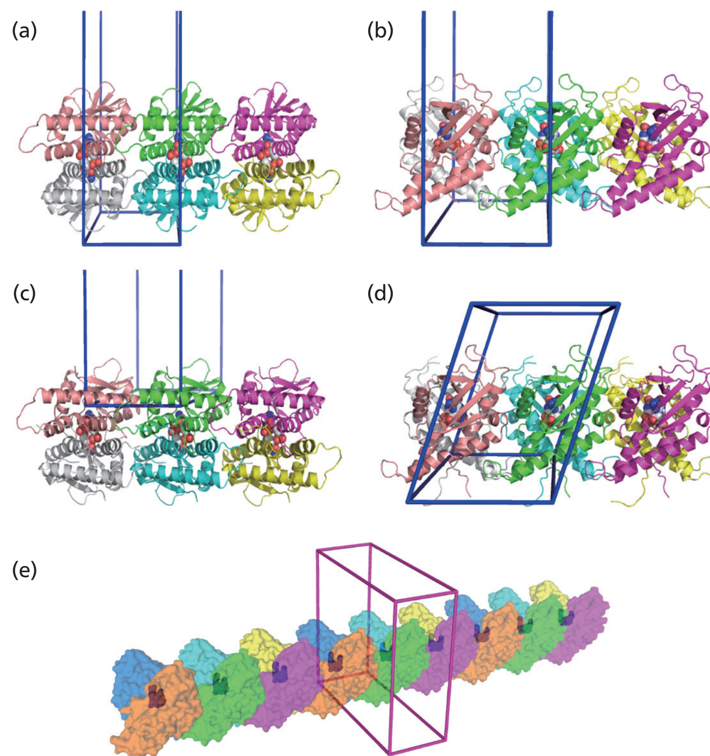

Fig. 2: Mode of bacterial STING oligomerization. Two orthogonal views of three juxtaposed dimers of *Pc*STING (a,b) and *My*STING (c,d) as viewed in crystals with color-differentiated protomers. The unit cells are depicted as cages. A diagram for the extended packing of the *Pc*STING crystal is depicted in (e) with color-differentiated translucent protein dimers. The bound CDG molecules are indicated in blue. [Reproduced from Ref. 3]

Structural Analysis and Engineering of Aldo-Keto Reductase from Glyphosate-Resistant *Echinochloa colona*

Glyphosate is the most widely used non-selective herbicide because of its high efficacy and low cost. Our study revealed the mechanism of aldo-keto reductase mediated glyphosate degradation and engineered a variant, which exhibited a 70% in glyphosate degradation.

Since it was first registered for use as a pesticide in 1974, glyphosate has become the most commonly used organophosphate herbicide. It acts as a 5-enolpyruvylshikimate-3-phosphate synthase inhibitor to block the shikimate pathway and aromatic amino acid biosynthesis.[1] In most plants, glyphosate can be degraded to weakly phytotoxic aminomethyl phosphonic acid and glyoxylate;[2] the underlying mechanisms of this process remain poorly understood. In 2020, a glyphosate-resistant *Echinochloa colona* (*E. colona*) population from western Australia has been reported.[3] The elevated glyphosate degradation in *E. colona* is caused by the upregulation of two homologous aldo–keto reductases (AKRs), namely AKR4C16 and AKR4C17.[3] AKR4C16 and AKR4C17 are the first naturally-occurring glyphosate-degrading machinery reported in plants.

To explore the mechanism of AKR-mediated glyphosate-degradation, a research team led by Rey-Ting Guo (Hubei University, China) solved the apo-form and cofactor/glyphosate-bound structures of AKR4C17 from the glyphosate-resistant *E. colona*.[4] The X-ray diffraction data were collected at **TLS 15A1** and **TPS 05A** of the NSRRC. AKR4C17 displays a triose-phosphate isomerase barrel

(TIM barrel) fold that consists of a central β-barrel surrounded by several helices (**Fig. 1(a)**). The protein harbors three large flexible loops (loop A, B, and C) on the top of the barrel, which are located close to the putative substrate entry site and are presumably related to substrate selectivity (**Fig. 1(a)**). Glyphosate was seen to be located adjacent to the nicotinamide moiety of the $NADP^+$ in a cavity that is formed by residues Trp21, Tyr49, Leu287, His111, Trp112, and Phe291 (**Fig. 1(b)**). The carboxylate group of glyphosate formed H-bond networks with Tyr49, His111, Trp21, and the O7N of $NADP^+$. The residues Leu287, Trp112, and Phe291 may provide hydrophobic interactions with glyphosate. Because the glyphosate observed in the structure is located near the catalytic tetrad and nicotinamide ring of $NADP^+$ where hydride transfer can take place, the cavity enclosing the glyphosate is presumed to be the authentic substrate-binding site. In addition, a variant F291D of AKR4C17 that was constructed based on structure-based engineering exhibited a 70% increase in glyphosate degradation (**Fig. 1(c)**).

AKRs are widely distributed in prokaryotes and eukaryotes and can be robustly classified into 16 subfamilies on the basis of sequence identity.[5] Members of families 1, 6, and 7 are found in humans and other mammals, whereas the majority of plant AKRs belongs to AKR4.[5] AKR4 includes A, B, and C subfamilies, with A playing a role in plant-microbe interactions, B in iron acquisition from the soil, and C in stress defense.[6,7] The research team also determined that residues that were responsible for glyphosate-binding were considerably conserved in AKR4C1–7 and 9–15.[4] Thus, these AKR members are expected to have the potential to degrade glyphosate as well as AKR4C17. This study provides molecular insights into the mechanism of action of AKR-mediated glyphosate degradation and greatly contribute to the deployment and application of glyphosate (Reported by Rey-Ting Guo, Hubei University, China).

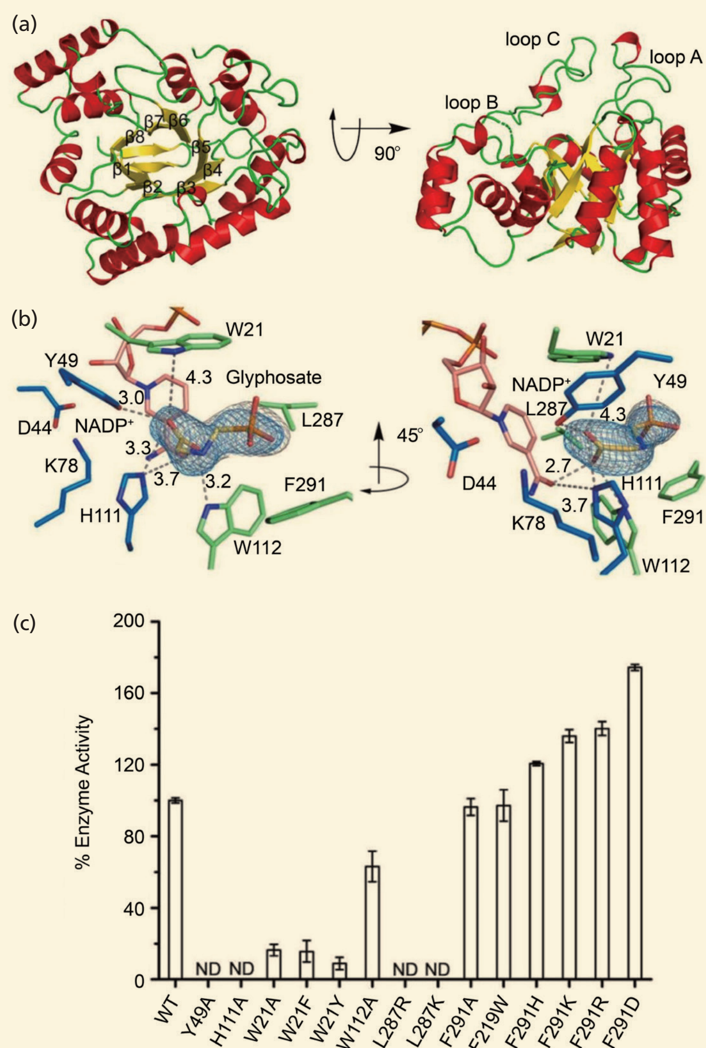

Fig. 1: Structural and functional investigation of the glyphosate-binding residues of AKR4C17. (a) The overall folding of AKR4C17, the α-helix, β-sheet, and loop region are colored red, yellow, and green, respectively. (b) The interaction network of AKR4C17 and glyphosate. The $2F_o–F_c$ (grey mesh) and $F_o–F_c$ omit (blue mesh) map of glyphosate were contoured at 1.0 and 3.0 σ, respectively. Glyphosate, $NADP^+$, catalytic-tetrad residues, and glyphosate-interacting residues are colored yellow, pink, blue, and green, respectively. The distances are labeled in the unit of Å. (c) The glyphosate-degrading activity of each mutant is presented as a percentage of wild-type AKR4C17. Each measurement was performed in triplicate. Error bars that indicate standard deviations are presented for each group. ND = not detectable. [Reproduced from Ref. 4]

This report features the work of Rey-Ting Guo and his collaborators published in J. Hazard. Mater. ***436****, 129191 (2022).*

TPS 05A Protein Microcrystallography
TLS 15A1 Biopharmaceuticals Protein Crystallography

- Protein Crystallography
- Biological Macromolecules, Protein Structures, Life Science

References

1. E. Schönbrunn, S. Eschenburg, W. A. Shuttleworth, J. V. Schloss, N. Amrhein, J. N. S. Evans, W. Kabsch, PNAS **98**, 1376 (2001).
2. T. A. Gaines, E. L. Patterson, P. Neve, New Phytol. **223**, 1770 (2019).
3. L. Pan, Q. Yu, H. Han, L. Mao, A. Nyporko, L. Fan, L. Bai, S. Powles, J. Plant Physiol. **181**, 1519 (2020).
4. H. Li, Y. Yang, Y. Hu, C. C. Chen, J. W. Huang, J. Min, L. Dai, R. T. Guo, J. Hazard. Mater. **436**, 129191 (2022).
5. T. M. Penning, Chem. Biol. Interact. **234**, 236 (2015).
6. J. M. Jez, M. J. Bennett, B. P. Schlegel, M. Lewis, T. M. Penning, Biochem. J. **326**, 625 (1997).
7. D. Sengupta, D. Naik, A. R. Reddy, J. Plant Physiol. **179**, 40 (2015).